# Palladium(0) Complexes of Diferrocenylmercury Diphosphines: Synthesis, X-ray Structure Analyses, Catalytic Isomerization, and C-Cl Bond Activation

Alain C. Tagne Kuate, a.b. Roger. A. Lalancette, Dirk Bockfeld, Matthias Tamm, and Frieder

Jäklea\*

<sup>a</sup> Department of Chemistry, Rutgers University-Newark, 73 Warren Street, Newark, NJ 07102, USA

<sup>b</sup> Department of Chemistry, Faculty of Sciences, University of Dschang, P.O. Box 67, Dschang,
Cameroon

<sup>c</sup> Institut für Anorganische und Analytische Chemie, Technische Universität Braunschweig, Hagenring 30, 38106 Braunschweig, Germany

\*To whom correspondence should be addressed. Email:  $\underline{fjaekle@rutgers.edu}$ 

**Abstract.** Palladium(0) phosphine complexes are of great importance as catalysts in numerous bond formation reactions that involve oxidative addition of substrates. Highly active catalysts with labile ligands are of particular interest but can be challenging to isolate and structurally characterize. We investigate here the synthesis and chemical reactivity of Pd<sup>0</sup> complexes that contain geometrically adaptable diferrocenylmercury-bridged diphosphine chelate ligands (L) in combination with a labile dibenzylideneacetone (dba) ligand. The diastereomeric diphosphines 1a (pSpR, meso-isomer) and 1b (pSpS-isomer) differ in the orientation of the ferrocene moiety relative to the central Ph<sub>2</sub>PC<sub>5</sub>H<sub>3</sub>-Hg-C<sub>5</sub>H<sub>3</sub>PPh<sub>2</sub> bridging entity. The structurally distinct trigonal LPd<sup>0</sup>(dba) complexes 2a (meso) and 2b (pSpS) are obtained upon treatment with Pd(dba)<sub>2</sub>. A competition reaction reveals that 1b reacts faster than 1a with Pd(dba)<sub>2</sub>. Unexpectedly, catalytic interconversion of **1a** (*meso*) into **1b** (*rac*) is observed at room temperature in the presence of only catalytic amounts of Pd(dba)<sub>2</sub>. Both Pd<sup>0</sup> complexes, **2a** and **2b**, readily undergo oxidative addition into the C-Cl bond of CH<sub>2</sub>Cl<sub>2</sub> at moderate temperatures with formation of the square planar transchelate complexes LPd<sup>II</sup>Cl(CH<sub>2</sub>Cl) (3a, 3b). Kinetic studies reveal a significantly higher reaction rate for the *meso*-isomer 2a in comparison to (pSpS)-2b.

### Introduction

Diphosphines play essential roles in homogeneous catalysis, and those ligands that are able to adapt to a preferred coordination environment during a catalytic process are of particular interest.<sup>1</sup> Only few diphosphines are known to be able to change the bite angle in a manner that allows them to adopt both *cis*- and *trans*-chelation modes.<sup>2</sup> Among them is the chiral diferrocenyldiphosphine PhTrap (Chart 1).<sup>3</sup> On the other hand, Z-type diphosphines that contain  $\sigma$ -acceptor atoms such as boron, aluminum, antimony, silicon, tin, zinc or mercury for secondary interactions with the metal

center are attracting much current interest.<sup>4</sup> An example is bis(*ortho*-diphosphinophenyl)mercury (DPHg, Chart 1).<sup>5</sup> DPHg has been reported to form a *trans*-chelate with Pd<sup>II</sup>Cl<sub>2</sub>, whereas both *cis*-and *trans*-chelates were isolated with Pt<sup>II</sup>Cl<sub>2</sub>.

**Chart 1.** Examples of adaptable diphosphines.

We have a longstanding interest in ferrocene-based Lewis acids and Lewis pairs provoked by the unique geometric features of ferrocene<sup>6</sup> that can be exploited in the development of planar chiral species<sup>7</sup> and the desirable redox-switchable<sup>8</sup> characteristics.<sup>9,10</sup> In the course of these studies we have recently introduced a new class of redox-active and planar-chiral diphosphines Hg(*ortho*-FcPPh<sub>2</sub>)<sub>2</sub> (**1a** and **1b**, Chart 1), which are formally related to PhTrap but linearly extended with a mercury atom that may act as a σ-acceptor unit.<sup>11</sup> These ligands are diastereomeric and, as illustrated in the formation of *trans*-chelated square planar Pd<sup>II</sup> complexes,<sup>11b</sup> they give rise to highly distinct complex geometries due to the different orientation of the 3-dimensional ferrocene moieties. The successful synthesis and unusual structures of these Pd<sup>II</sup> complexes prompted us to further explore **1a** and **1b** as ligands for Pd complexes in the oxidation state of zero. Highly active Pd<sup>0</sup> complexes that readily undergo oxidative addition of substrates are of significant interest,<sup>12</sup>

especially the complexes derived from Pd(dba)<sub>2</sub> or Pd<sub>2</sub>(dba)<sub>3</sub> in combination with phosphine ligands have proven to be very effective. They are typically generated *in-situ*, and only relatively few examples of structurally authenticated active complexes have been reported in the literature.<sup>13</sup>

In here we report the formation of low-coordinate trigonal complexes LPd $^0$ (dba) (L = 1a or 1b, dba = dibenzylideneacetone) that are readily isolable and structurally characterized by single crystal X-ray analysis. We further disclose that these Pd $^0$  complexes rapidly insert into the C-Cl bond of CH<sub>2</sub>Cl<sub>2</sub>, thereby exemplifying their potential utility in bond activation processes. Intriguingly, the rate of formation of the LPd $^0$ (dba) complexes, the geometric features of the complexes, and their reactivity toward CH<sub>2</sub>Cl<sub>2</sub>, are found to vary significantly with the ligand stereochemistry.

### **Results and Discussion**

The diferrocenylmercury-bridged diphosphines meso-1a and (pS,pS)-1b were prepared as previously reported. Upon stirring 1a with Pd(dba)<sub>2</sub> in a 1:1 molar ratio in toluene for 30 min at room temperature, the Pd<sup>0</sup> complex 2a was obtained in 82% yield and a similar reaction with chiral (pS,pS)-1b gave the isomer (pS,pS)-2b in 86% yield (Scheme 1). The enantiomeric enrichment of (pS,pS)-2b was verified by optical rotation measurement ( $[\alpha]^{20}_D = +414$  in toluene). The conversion to the Pd<sup>0</sup> complexes is evidenced by new resonances in the  $^{31}P$  NMR spectra in C<sub>6</sub>D<sub>6</sub> at  $\delta = 20.9$  (2a) and 18.1 ppm ((pS,pS)-2b), respectively, that are low-field shifted by  $\Delta \delta = 31.6$  and 33.9 ppm relative to those of the free ligands. For each isomer one of the dba ligands remains bound to Pd as evidenced by the presence of doublets due to the olefinic protons of the benzylidene moieties at  $\delta = 7.73/6.82$  ppm ( $^2J_{H,H} = 16$  Hz) for 2a and at  $\delta = 7.71/6.76$  ppm ( $^2J_{H,H} = 15$  Hz) for (pS,pS)-2b. High-resolution MS analyses revealed peaks at m/z = 1045.9731 Da ( $[2a]^+$ , MALDI-MS) and 1046.9868 ( $[2b+H]^+$ , ESI-MS) that correspond to loss of the dba ligand and are consistent

with the diastereomeric relationship. Slow evaporation of a solution in benzene/decane (2a) or toluene/decane (2b) gave single crystals appropriate for analysis by X-ray diffraction (Figure 1). The molecular structure of 2a exhibits disorder occurring at the dba ligand (Figure S1, SI).

Scheme 1. Synthesis of Pd<sup>0</sup> complexes 2a and 2b.

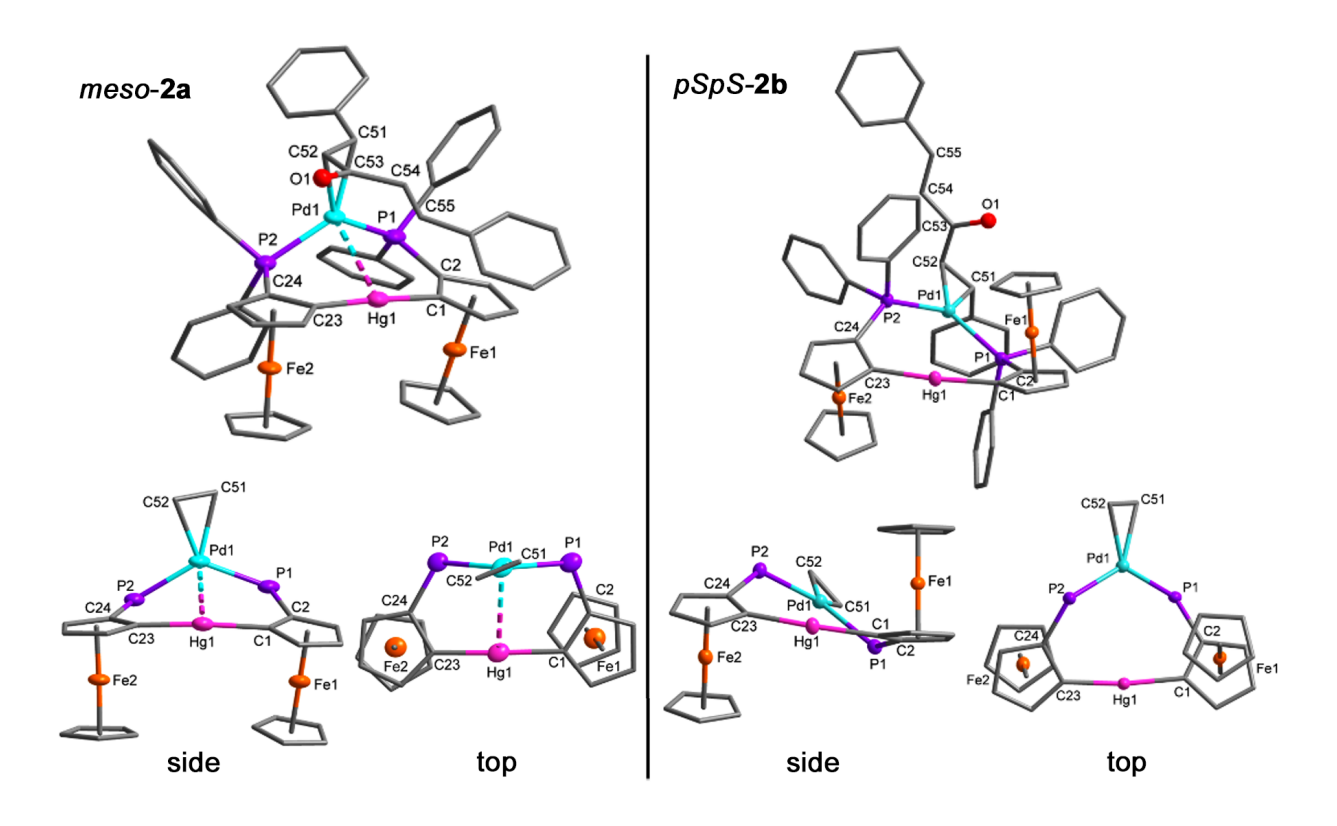


**Figure 1.** Molecular structures of **2a** and **2b** (50% thermal ellipsoids, H atoms omitted for clarity) and side and top views with Ph groups on P omitted and only the Pd-bound olefin of the dba ligand shown. Selected interatomic distances (Å) and angles (°): For **2a**: Pd1–P1 2.327(3), Pd1–P2 2.346(3), Pd1–C51 2.198(12), Pd1–C52 2.197(10), Pd1···Hg1 3.0381(10), Hg1–C1 2.070(12), Hg1–C23 2.047(13), P1–C2 1.815(11), P2–C24 1.825(12), C51–C52 1.40(2), C1–Hg1–C23 175.6(4), P1–Pd–P2 126.57(11), dihedral angle for substituted Cp//Cp 15.9. For **2b**: Pd1–P1 2.366(2), Pd1–P2 2.362(2), Pd1–C51 2.220(9), Pd1–C52 2.181(8), Pd1····Hg1 3.9056, Hg1–C1 2.055(7), Hg1–C23 2.050(7), P1–C2 1.833(8), P2–C24 1.815(8), C51–C52 1.402(12), C54–C55 1.337(13), C53-O1 1.228(11), C1–Hg1–C23 174.1(3), P1–Pd–P2 127.53(7), dihedral angle for substituted Cp//Cp 29.7.

The Pd<sup>0</sup> atom in 2a and 2b is found in a trigonal planar environment surrounded by the chelating diphosphine ligand and one of the olefinic groups of the dba ligand. The P1-Pd-P2 bite angles of 126.57(11)° for 2a and 127.53(7)° for 2b are much smaller than in the previously reported LPd<sup>II</sup>Cl<sub>2</sub> complexes, 11b which demonstrates the highly flexible nature of this class of ligands. The arrangement of the ferrocene units in the two metal complexes drastically influences the positioning of the Pd(dba) fragment, which is aligned in a way that minimizes steric repulsion with the ferrocene groups and phenyl rings. The Pd(dba) unit sits above the diferrocenylmercury entity in 2a but is oriented perpendicular to the diferrocenylmercury entity in 2b. The repulsion between the dba and ferrocene units (and the Ph rings that are differently oriented) positions the Pd in **2b** far away from the Hg atom (Pd···Hg 3.9056 Å) and induces an elongation of the Pd–P bond lengths (2.366(2) and 2.362(2) Å), in sharp contrast to the short interatomic Pd···Hg separation (3.0381(10) Å) and relatively shorter Pd-P distances (2.327(3) and 2.346(3) Å) observed for 2a. For a similarly short Pd···Hg distance to be realized for 2b, the Pd would have to adopt a T-shaped geometry due to the different orientation of the P<sub>2</sub>Pd plane. The substituted Cp rings deviate from coplanarity with a twist of 15.9° (2a) and 29.7° (2b) that results in a more

puckered C<sub>4</sub>HgPdP<sub>2</sub> central heterocycle for the latter. The Pd–P1 and Pd–P2 distances in both species are shorter than those reported for Pd(dba)[P(o-tol)<sub>3</sub>]<sub>2</sub> (2.372(1) and 2.388(1) Å),<sup>13a</sup> suggesting that the phosphorus atoms are more tightly bound to Pd in the chelate complexes **2a** and **2b**. As expected, the C–C distance for the Pd-bound olefinic group [1.40(2) Å for **2a**; 1.402(12) for **2b**] is elongated when compared with the corresponding unbound olefin in free dba (1.276(4)/1.289(6) Å)<sup>14</sup>.

The short Pd···Hg distance of 3.0381(10) Å in **2a** deserves some additional comments as it may be indicative of d¹¹¹-d¹¹ metallophilic interactions. Although metallophilic interactions involving Pd<sup>II</sup> (d<sup>8</sup>) complexes are very common and have been extensively studied,<sup>5,11b,15</sup> they are relatively less explored for Pd¹ (d¹¹) complexes.¹¹ The nature and strength of such interactions remain the subject of vigorous debate with recent studies emphasizing the importance of ligand effects that can overcome even repulsive M···M interactions.¹¹ In line with this view, the presence of a short Pd···Hg contact in **2a** and absence in **2b** is certainly tied to the different ligand environments.

To evaluate any differences in reactivity between isomers  $\bf 1a$  and  $\bf 1b$ , a competition experiment was performed using an approximately equimolar mixture of each of the diphosphine diastereomers and Pd(dba)<sub>2</sub>. Immediately after mixing  $\bf 1a$ ,  $\bf 1b$ , and Pd(dba)<sub>2</sub> in a 1:1:1 ratio in C<sub>6</sub>D<sub>6</sub> the <sup>31</sup>P NMR spectrum displayed low field resonances for the expected products at  $\delta = 21.5$  (10%,  $\bf 2a$ ) and 17.6 (36%,  $\bf 2b$ ), in addition to high field resonances at -12.7 ppm (40%,  $\bf 1a$ ), and -13.3 (13%,  $\bf 1b$ ) for the precursors (Figure 2, Spectrum 1). The preferential reaction of  $\bf 1b$  over  $\bf 1a$  suggests a lower kinetic barrier for the binding of  $\bf 1b$  to the Pd(dba) fragment.

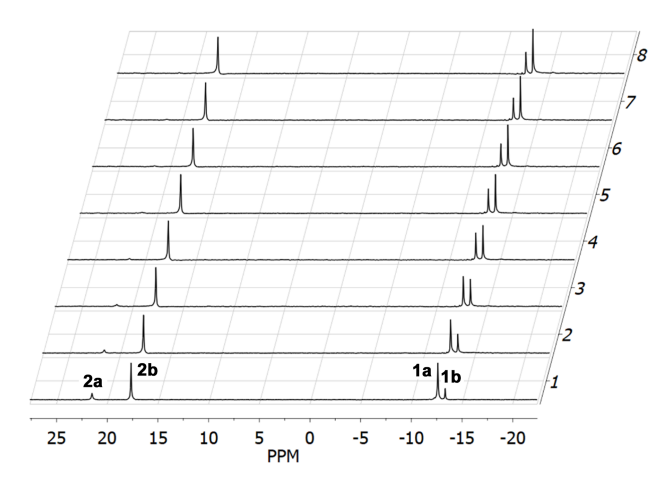


**Figure 2.** <sup>31</sup>P NMR spectra for the competitive 1:1:1 reaction of **1a**:**1b**:Pd(dba)<sub>2</sub> in C<sub>6</sub>D<sub>6</sub>; spectrum 1 was acquired immediately after mixing and subsequent spectra (2–8) were recorded every 30 min.

Looking at the differences in the X-ray structure of **2a** and **2b**, a possible explanation may be that, in the formation of **2a**, the Pd(dba) moiety has to approach from above the diferrocenyl mercury moiety, interfering with the Ph groups of the phosphine ligands, whereas in the formation of **2b** the Pd(dba) moiety can approach sideways and retains a larger distance to the diferrocenylmercury core in the final metal complex. A detailed analysis of the percent buried volume<sup>18</sup> and corresponding steric maps of the ligands are provided in the ESI (Figure S2).

When the sample was kept at room temperature for a longer period of time, the relative intensity of the signals for *meso*-isomers **2a** and **1a** gradually decreased, while those of the signals for *pSpS*-isomers **2b** and **1b** increased (Figure 2, Spectra 2–8). After a reaction time of 4 h, **2a** completely disappeared and the relative intensity of **1a**, **1b**, and **2b** were respectively 17%, 39%, and 44%. These results suggest that a rearrangement reaction occurred that favored the formation of the free ligand **1b** and its metal complex **2b**. To further explore this phenomenon, we added a catalytic amount of Pd(dba)<sub>2</sub> (ca. 15 mol%) to a solution of the *meso- and rac-*isomers **1a** and **1b** 

(starting isomer ratio 84%: 16% for **1a**: **1b**) in C<sub>6</sub>D<sub>6</sub>. Indeed, the <sup>31</sup>P NMR data showed a gradual increase of the signal for the *rac*-isomer **1b** and decrease of the signal for the *meso*-isomer **1a** (Figure S4). After 29 hours at room temperature, the free ligand ratio of **1a** to **1b** changed to 38%: 45%, with the remaining 17% attributed to the Pd complex **2b**. The isomerization mechanism remains unclear but inevitably has to involve mercuration at the Cp C-H carbon in *ortho*-position to the PPh<sub>2</sub> ligand binding group and transfer of the proton from that position to the Cp carbon atom that originally was substituted with Hg. Further studies will be needed to elucidate the mechanistic details.

C–Cl Bond Activation of Dichloromethane. An excess of dichloromethane was added to a Schlenk flask containing **2a** and the mixture was stirred overnight at 40 °C. Analysis by NMR spectroscopy revealed almost complete, clean conversion to **3a** (Figure 3). A similar procedure led to the formation of **3b** in high yield. The <sup>31</sup>P NMR spectrum of **3a** exhibits a resonance at  $\delta = 25.1$  ppm, which is shifted to lower field in comparison with that measured for **2a**, while the chloromethyl protons give rise to a sharp triplet resonance at  $\delta = 2.51$  ppm ( $^3J_{P,H} = 10.0 \text{ Hz}$ ). In contrast, the <sup>31</sup>P NMR spectrum of **3b** shows two doublets centered at  $\delta = 24.6$  ppm and 20.7 ppm ( $^2J_{P,P} = 405 \text{ Hz}$ )<sup>20</sup> indicating two magnetically non-equivalent phosphorus atoms as a result of a change from  $C_2$ - in **2b** to  $C_1$ -symmetry in **3b** upon activation of CH<sub>2</sub>Cl<sub>2</sub>. As another consequence, the chloromethyl protons are diastereotopic and appear as two distinct broad resonances in the <sup>1</sup>H NMR spectrum at  $\delta = 3.02$  and 2.93 ppm.

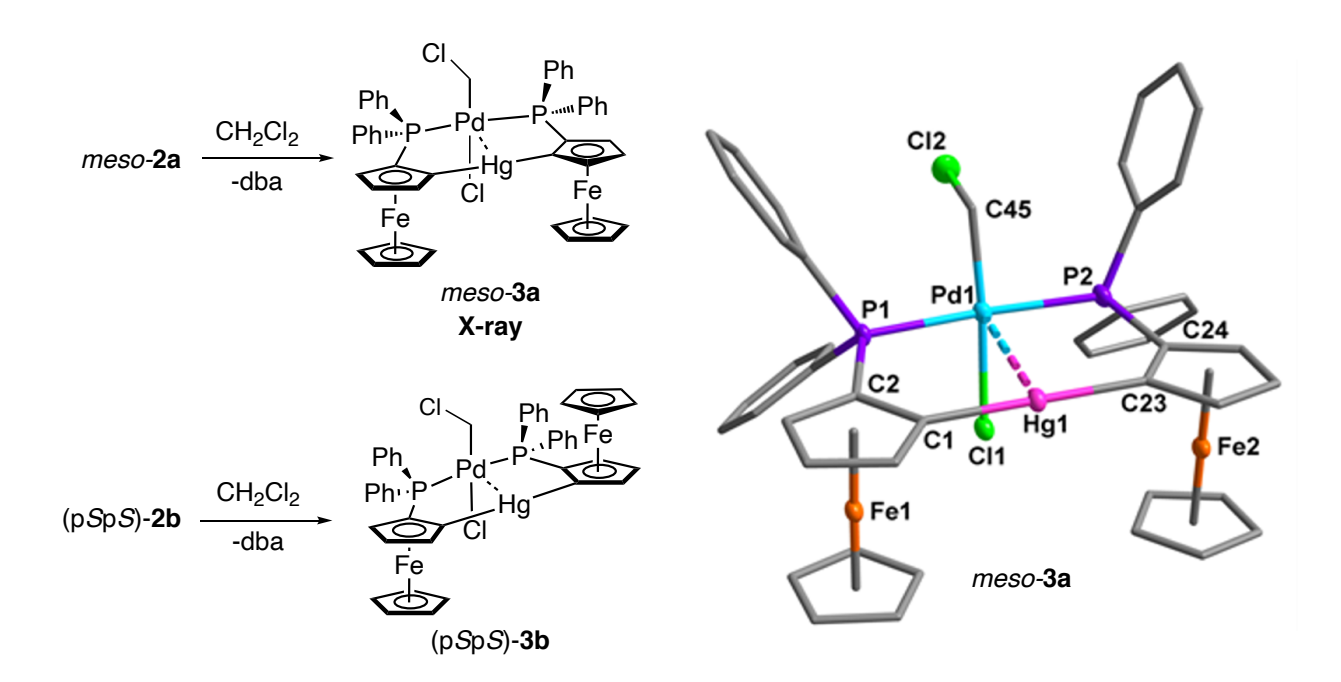


**Figure 3.** C–Cl bond activation of dichloromethane at the Pd<sup>0</sup> complexes **2a** and **2b** to give **3a** and **3b** and molecular structure of *meso-***3a**·2CH<sub>2</sub>Cl<sub>2</sub> (50% ellipsoids, H atoms and CH<sub>2</sub>Cl<sub>2</sub> solvent molecules omitted for clarity). Selected interatomic distances (Å) and angles (°): Pd1–P1 2.3376(17), Pd1–P2 2.3591(17), Pd1–Cl1 2.4016(15), Pd1–C45 2.038(6), Pd1···Hg1 2.9784(10), P1–C2 1.799(6), P2–C24 1.805(6), Hg1–C1 2.066(6), Hg1–C23 2.077(6), C45–Cl2 1.811(6), C1–Hg1–C23 179.0(2), P1–Pd–P2 173.29(5), C11–Pd1–C45 174.70(18), Pd1–C45–Cl2 105.9(3), dihedral angle for substituted Cp//Cp 2.1.

Single crystals of the Pd<sup>II</sup> complex  $\bf 3a$  were obtained by slow evaporation of a CH<sub>2</sub>Cl<sub>2</sub> solution of  $\bf 2a$  layered with hexanes, which resulted in a mixture of orange and light-yellow crystals. While the light-yellow crystals were identified as the dba ligand, the orange crystals proved to correspond to  $\bf 3a$  as confirmed by X-ray diffraction analysis (Figure 3, right).  $\bf 3a$  adopts a structure similar to that of the previously reported complex LPd<sup>II</sup>Cl<sub>2</sub> (L = (Ph<sub>2</sub>Pfc)Hg)<sup>11b</sup> with the Pd atom *trans*-coordinated by two phosphine groups, which in turn adopt a *cis*-arrangement relative to the Fc<sub>2</sub>Hg entity. The P1–Pd1–P2 (173.29(5)°) and Cl1–Pd1–C45 (174.70(18)°) angles of  $\bf 3a$  are slightly

smaller than those of LPd<sup>II</sup>Cl<sub>2</sub>, whereas the Pd1···Hg1 distance (2.9784(10) Å) in **3a** is in a similar range as that of LPd<sup>II</sup>Cl<sub>2</sub> (Pd1···Hg1 2.9828(6) Å)<sup>11b</sup>. The latter may indicate the presence of metallophilic d<sup>8</sup>-d<sup>10</sup> interactions as the distance is well below that of most compounds<sup>15</sup> for which Pd···Hg d<sup>8</sup>-d<sup>10</sup> interactions have previously been claimed [3.1020(3)–3.2841(2) Å].

An interesting question is whether the distinct steric features and the presence/absence of short Hg...Pd contacts for the Pd<sup>0</sup> complexes 2a and 2b may also affect the rate of the CH<sub>2</sub>Cl<sub>2</sub> oxidative addition. To assess potential differences in the reaction kinetics, we performed a study in which we followed the reaction of a 1:1 mixture of 2a and 2b by <sup>31</sup>P NMR in a mixture of CH<sub>2</sub>Cl<sub>2</sub> (40%) and C<sub>6</sub>D<sub>6</sub> (60%) at 40 °C (Figure 4a). After 40 min, the concentration of the meso-isomer 2a decreased by 22% and the corresponding signal for 3a was easily detected. In contrast, the concentration of the rac-isomer 2b decreased only slightly and the doublet signals for the product **3b** remained barely detectable. As the reaction progressed, the difference in reactivity became even more apparent. A plot of the ln[2a] and ln[2b] versus time showed that the reaction follows a firstorder rate law. Considering that the amount of CH<sub>2</sub>Cl<sub>2</sub> (6.26 M) remains constant, the rate constants were determined to be  $5.0 \times 10^{-2} \,\mathrm{M}^{-1} \,\mathrm{s}^{-1}$  (2a) and  $3.2 \times 10^{-2} \,\mathrm{M}^{-1} \,\mathrm{s}^{-1}$  (2b) (Figure 4b). The apparent lower propensity of 2b to insert into the C-Cl bond of dichloromethane is indicative of a larger barrier to oxidative addition for 2b. A reason could be that the more asymmetric structure of 2b hinders the oxidative addition at the Pd<sup>0</sup> center. While the initial approach of DCM to Pd should occur readily, the DCM molecule likely approaches sideways as seen for the binding of dba in 2b, resulting in a longer Hg...Pd distance. Subsequent oxidative addition with formation of the square-planar product then requires the Pd to approach more closely to the diferrocenylmercury ligand framework which may be associated with a relatively higher reaction barrier.

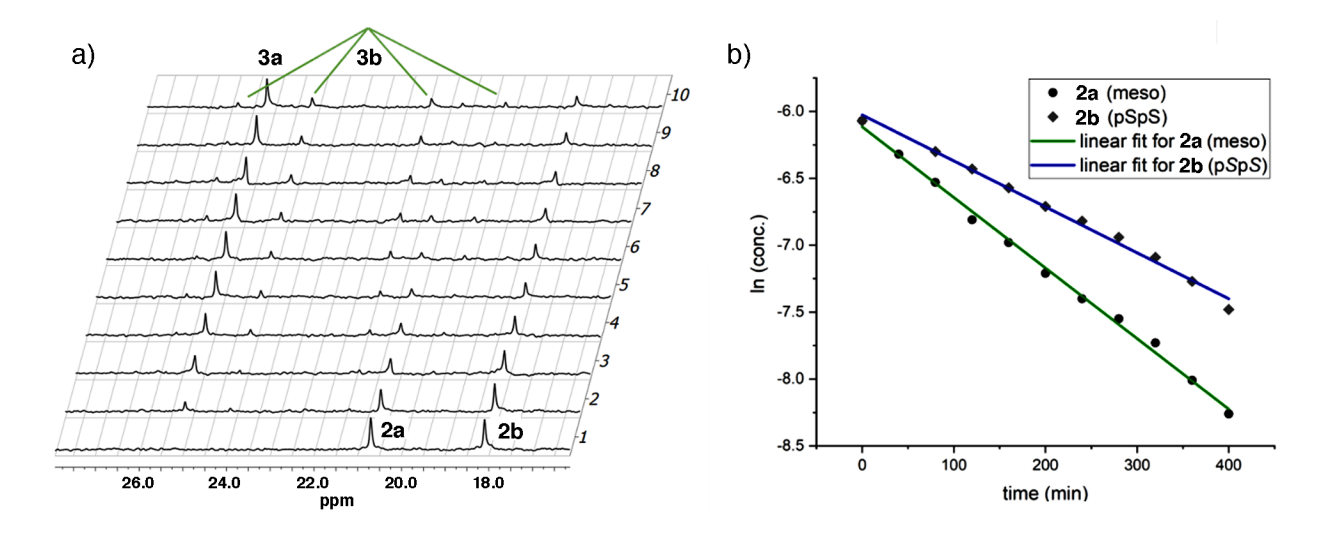


**Figure 4.** (a) Activation of CH<sub>2</sub>Cl<sub>2</sub> by *meso-***2a** and (pSpS)-**2b** (1:1 mixture) followed by  $^{31}$ P NMR at 40  $^{\circ}$ C (spectrum 1 shows the starting materials at t = 0 min and subsequent spectra (2–10) were acquired every 40 minutes). (b) Logarithmic plot showing the decrease in concentration of **2a** and **2b** versus time.

The facile dichloromethane activation at ambient temperature by **2a** and **2b** merits some further comments. Owing to its high stability, activation of dichloromethane by transition metal insertion into the C–Cl bond generally requires the use of highly reactive, electron-rich transition metal complexes.<sup>21</sup> Literature precedents for activation of CH<sub>2</sub>Cl<sub>2</sub> with Pd<sup>0</sup> are mostly limited to electron-rich monophosphine metal complexes such as [Pd(PtBu<sub>2</sub>H)<sub>3</sub>]<sup>22</sup> and [Pd(PCy<sub>3</sub>)<sub>2</sub>(dba)]<sup>23</sup> which give rise to square-planar *trans*-complexes.<sup>24</sup> A square-planar *cis*-complex [Pd(Cy<sub>2</sub>PC<sub>2</sub>H<sub>4</sub>PCy<sub>2</sub>)(CH<sub>2</sub>Cl)Cl] (Pd–C 2.101(9), Pd–Cl 2.398(2) Å) was obtained upon reaction of the chelate ligand Cy<sub>2</sub>PC<sub>2</sub>H<sub>4</sub>PCy<sub>2</sub> with the methallyl complex Pd(η<sup>3</sup>-2-Me-C<sub>3</sub>H<sub>4</sub>)<sub>2</sub> in CH<sub>2</sub>Cl<sub>2</sub>.<sup>25</sup> Most closely related is a study by Mashima and co-workers on a tetranuclear Pd(0)-Mo(II)-Mo(II)-Pd(0) complex in which the Pd atoms are surrounded by trans-chelating phosphines and show dative interactions with the Mo atoms that are part of the diphosphine backbone.<sup>26</sup> This compound was reported to be highly reactive to oxidative addition, also undergoing CH<sub>2</sub>Cl<sub>2</sub> oxidative addition

at room temperature. In addition, Hierso and Lucas introduced a bidentate ferrocenylphosphine ligand and demonstrated that its electrochemically generated Pd<sup>0</sup> complex rapidly reacts with CH<sub>2</sub>Cl<sub>2</sub>.<sup>27</sup> In the resulting square-planar Pd<sup>II</sup> complex, the CH<sub>2</sub>Cl and Cl groups are found in *cis*-position (Pd–C 2.065(5), Pd–Cl 2.357(4) Å) and the product is reported to be unstable towards loss of "methylene". In contrast, both compounds **3a** and **3b** are stable in solution for many days (the NMR sample resulting from the kinetic experiment was kept for five days at room temperature)

and no loss of "methylene" with formation of the respective LPd<sup>II</sup>Cl<sub>2</sub> complexes<sup>11b</sup> was observed.

### **Conclusions**

In conclusion, reaction of the diphosphines *meso-1a* and (pS,pS)-1b with Pd(dba)<sub>2</sub> gives rise to the novel Pd<sup>0</sup> complexes *meso-2a* and (pS,pS)-2b. The metal complexes adopt a trigonal coordination geometry at Pd, in contrast to the square-planar arrangement for the respective LPd<sup>II</sup>Cl<sub>2</sub> complexes, highlighting the conformational flexibility of the ligands. Distinct geometries are observed for *meso-2a* and (pS,pS)-2b that are reflected in dramatic differences in the coordination geometry at Pd and also affect the establishment of short intramolecular Pd···Hg contacts. Likely due to these differences, in competitive reactions 1b reacts preferentially over 1a with the palladium precursor Pd(dba)<sub>2</sub>. In the course of these studies we also discovered that 1a is slowly converted to 1b catalyzed by Pd(dba)<sub>2</sub>. Both Pd<sup>0</sup> complexes, 2a and 2b, undergo C-Cl activation of CH<sub>2</sub>Cl<sub>2</sub> under mild conditions to give LPd<sup>II</sup>Cl(CH<sub>2</sub>Cl) complexes, 3a and 3b. Kinetic studies indicate a relatively higher reactivity of the Pd<sup>0</sup> species 2a in comparison to 2b. The high propensity to undergo oxidative addition processes suggests that the Pd<sup>0</sup> complexes hold promise for other transition metal-catalyzed transformations including stereoselective processes.

**Conflicts of interest:** There are no conflicts of interest to report.

Acknowledgements: A.C.T.K. thanks the Deutsche Forschungsgemeinschaft (DFG) for a postdoctoral fellowship. A 500 MHz NMR spectrometer used in these studies was purchased with support from the NSF-MRI program (1229030). The Bruker SMART APEX II X-ray diffractometer was purchased with support from the NSF-CRIF program (0443538) and Rutgers University (Academic Excellence Fund). Access to a Rigaku XtaLAB Synergy S diffractometer was provided by the Technische Universität Braunschweig.

## References

- 1. J. A. Gillespsie, E. Zuidema, P. W. N. M. Leuwen, P. C. J. Kamer, *Phosphorus Ligand Effects in Homogenous Catalysis and Rational Catalyst Design, in Phosphorus(III) Ligands in Homogeneous Catalysis: Design and Synthesis*, 1st Edition, P. C. J. Kamer and P. W. N. M. Leuwen, eds.; Wiley, 2012.
- a) P. W. N. M. van Leeuwen, P. C. J. Kamer, J. N. H. Reek and P. Dierkes, *Chem. Rev.*, 2000, 100, 2741-2769; b) W. J. van Zeist, R. Visser and F. M. Bickelhaupt, *Chem. Eur. J.*, 2009, 15, 6112-6115;
   c) B. J. Barrett and V. M. Iluc, *Organometallics*, 2017, 36, 730-741.
- 3. M. Sawamura, H. Hamashima, M. Sugawara, R. Kuwano and Y. Ito, *Organometallics*, 1995, **14**, 4549-4558.
- a) A. Amgoune and D. Bourissou, *Chem. Commun.*, 2011, 47, 859-871; b) H. Braunschweig and R. D. Dewhurst, *Dalton Trans.*, 2011, 40, 549-558; c) G. Bouhadir and D. Bourissou, *Chem. Soc. Rev.*, 2016, 45, 1065-1079; d) J. S. Jones and F. P. Gabbaï, *Acc. Chem. Res.*, 2016, 49, 857-867; e) J. W. Taylor, A. McSkimming, M. E. Moret and W. H. Harman, *Angew. Chem. Int. Ed.*, 2017, 56, 10413-10417; f) D. You and F. P. Gabbai, *Trends Chem.*, 2019, 1, 485-496; g) F. M. Miloserdov, C. J. Isaac, M. L. Beck, A. L. Burnage, S. A. M. James C. B. Farmer, M. F. Mahon and M. K. Whittlesey, *Inorg. Chem.*, 2020, 59, 15606-15619.
- a) M. A. Bennett, M. Contel, D. C. R. Hockless and L. L. Welling, *Chem. Commun.*, 1998, 2401-2402;
  b) M. A. Bennett, M. Contel, D. C. R. Hockless, L. L. Welling and A. C. Willis, *Inorg. Chem.*, 2002, 41, 844-855.
- a) A. Togni and T. Hayashi, eds., Ferrocenes, VCH, Weinheim, New York, Basel, Cambridge, Tokyo,
   1995; b) C. Nataro, in Reference Module in Chemistry, Molecular Sciences and Chemical Engineering, Elsevier, 2019.
- 7. R. G. Arrayas, J. Adrio and J. C. Carretero, *Angew. Chem., Int. Ed.*, 2006, **45**, 7674-7715.

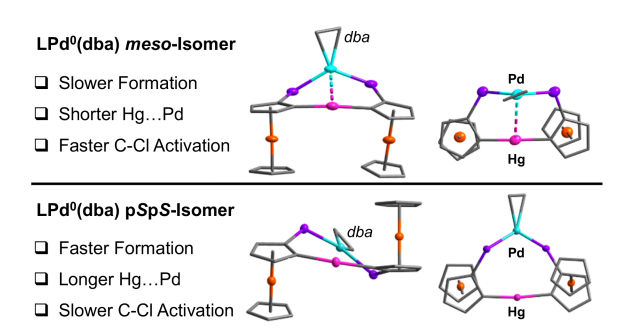
- a) P. Štěpnička, Ferrocenes: Ligands, Materials and Biomolecules, Wiley, Chichester, U.K.,, 2008;
  b) K. Venkatasubbaiah, I. Nowik, R. H. Herber and F. Jäkle, Chem. Commun., 2007, 2154-2156;
  c) J. N. Wei and P. L. Diaconescu, Acc. Chem. Res., 2019, 52, 415-424.
- a) J. A. Gamboa, A. Sundararaman, L. Kakalis, A. J. Lough and F. Jäkle, *Organometallics*, 2002, 21, 4169-4181; b) K. Venkatasubbaiah, J. W. Bats, A. L. Rheingold and F. Jäkle, *Organometallics*, 2005, 24, 6043-6050; c) R. Boshra, A. Sundararaman, L. N. Zakharov, C. D. Incarvito, A. L. Rheingold and F. Jäkle, *Chem. Eur. J.*, 2005, 11, 2810-2824; d) K. Venkatasubbaiah, L. N. Zakharov, W. S. Kassel, A. L. Rheingold and F. Jäkle, *Angew. Chem. Int. Ed.*, 2005, 44, 5428-5433; e) R. Boshra, A. Doshi and F. Jäkle, *Angew. Chem. Int. Ed.*, 2008, 47, 1134-1137; f) J. Chen, K. Venkatasubbaiah, T. Pakkirisamy, A. Doshi, A. Yusupov, Y. Patel, R. A. Lalancette and F. Jäkle, *Chem. Eur. J.*, 2010, 16, 8861-8867; g) J. W. Chen, R. A. Lalancette and F. Jäkle, *Organometallics*, 2013, 32, 5843-5851; h) J. W. Chen, R. A. Lalancette and F. Jäkle, *Chem. Eur. J.*, 2014, 20, 9120-9129; j) J. W. Chen, D. A. M. Parra, R. A. Lalancette and F. Jäkle, *Angew. Chem. Int. Ed.*, 2015, 54, 10202-10205; k) J. Chen, A. C. T. Kuate, R. A. Lalancette and F. Jäkle, *Organometallics*, 2016, 35, 1964-1972; l) A. C. Tagne Kuate, R. A. Lalancette and F. Jäkle, *Dalton Trans.*, 2017, 46, 6253-6264.
- a) K. B. Ma, M. Scheibitz, S. Scholz and M. Wagner, J. Organomet. Chem., 2002, 652, 11-19; b) M. Scheibitz, M. Bolte, J. W. Bats, H. W. Lerner, I. Nowik, R. H. Herber, A. Krapp, M. Lein, M. C. Holthausen and M. Wagner, Chem.—Eur. J., 2005, 11, 584-603; c) M. J. Kelly, J. Gilbert, R. Tirfoin and S. Aldridge, Angew. Chem. Int. Ed., 2013, 52, 14094-14097; d) S. R. Tamang, J.-H. Son and J. D. Hoefelmeyer, Dalton Trans., 2014, 43, 7139-7145; e) B. E. Cowie and D. J. H. Emslie, Organometallics, 2015, 34, 4093-4101; f) E. Lerayer, P. Renaut, S. Brandes, H. Cattey, P. Fleurat-Lessard, G. Bouhadir, D. Bourissou and J. C. Hierso, Inorg. Chem., 2017, 56, 1966-1973; g) B. E. Cowie and D. J. H. Emslie, Organometallics, 2018, 37, 1007-1016; h) E. Lerayer, P. Renaut, J. Roger,

- N. Pirio, H. Cattey, P. Fleurat-Lessard, M. Boudjelel, S. Massou, G. Bouhadir, D. Bourissou and J. C. Hierso, *Dalton Trans.*, 2019, **48**, 11191-11195; i) H. Bhattacharjee, J. F. Zhu and J. Müller, *Angew. Chem. Int. Ed.*, 2019, **58**, 16575-16582; j) M. P. T. Cao, J. W. Quail, J. F. Zhu and J. Müller, *Organometallics*, 2019, **38**, 2092-2104.
- a) A. C. Tagne Kuate, R. A. Lalancette, T. Bannenberg and F. Jäkle, *Angew. Chem. Int. Ed.*, 2018, **57**, 6552-6557; b) A. C. Tagne Kuate, R. A. Lalancette, T. Bannenberg, M. Tamm and F. Jäkle, *Dalton Trans.*, 2019, **48**, 13430-13439; c) A. C. Tagne Kuate, R. A. Lalancette and F. Jäkle, *Organometallics*, 2019, **38**, 677-687.
- a) P. Frederic, J. Patt and J. F. Hartwig, *Organometallics*, 1995, 14, 3030-3039; b) C. Y. Dai and G. C. Fu, *J. Am. Chem. Soc.*, 2001, 123, 2719-2724; c) P. G. Gildner and T. J. Colacot, *Organometallics*, 2015, 34, 5497-5508; d) P. Weber, A. Biafora, A. Doppiu, H. J. Bongard, H. Kelm and L. J. Goossen, *Org. Process Res. Dev.*, 2019, 23, 1462-1470; e) E. D. Slack, P. D. Tancini and T. J. Colacot, in *Organometallics in Process Chemistry*, eds. T. J. Colacot and V. Sivakumar, Springer International Publishing, Cham, 2019, pp. 161-198.
- a) B. A. Harding, P. R. Melvin, W. Dougherty, S. Kassel and F. E. Goodson, *Organometallics*, 2013,
  32, 3570-3573; b) E. Janusson, H. S. Zijlstra, P. P. T. Nguyen, L. MacGillivray, J. Martelino and J. S. McIndoe, *Chem. Commun.*, 2017, 53, 854-856; c) P. Steinhoff, M. Paul, J. P. Schroers and M. E. Tauchert, *Dalton Trans.*, 2019, 48, 1017-1022; d) H. Kameo, J. Yamamoto, A. Asada, H. Nakazawa, H. Matsuzaka and D. Bourissou, *Angew. Chem. Int. Ed.*, 2019, 58, 18783-18787.
- 14. Free dba released from the oxidative addition of DCM (vide infra) was analyzed by X-ray diffraction analysis. The molecular structure shows a C=C bond length of 1.315(9) Å; see: I. Turowska-Tyrk, Chem. Phys., 2003, 288, 241-247.
- a) L. R. Falvello, J. Fornies, A. Martin, R. Navarro, V. Sicilia and P. Villarroya, *Inorg. Chem.*, 1997,
   36, 6166-6171; b) L. R. Falvello, S. Fernandez, R. Navarro and E. P. Urriolabeitia, *Inorg. Chem.*,

- 1999, **38**, 2455-2463; c) M. Kim, T. J. Taylor and F. P. Gabbaï, *J. Am. Chem. Soc.*, 2008, **130**, 6332-6333; d) S. Sharma, R. S. Baligar, H. B. Singh and R. J. Butcher, *Angew. Chem. Int. Ed.*, 2009, **48**, 1987-1990; e) S. Raju, H. B. Singh and R. J. Butcher, *Dalton Trans.*, 2020, **49**, 9099-9117.
- a) Y. L. Pan, J. T. Mague and M. J. Fink, *J. Am. Chem. Soc.*, 1993, 115, 3842-3843; b) P. F. Ai, K. Y.
   Monakhov, J. van Leusen, P. Kogerler, C. Gourlaouen, M. Tromp, R. Welter, A. A. Danopoulos and
   P. Braunstein, *Chem.–Eur. J.*, 2018, 24, 8787-8796.
- a) Q. S. Zheng, S. Borsley, G. S. Nichol, F. Duarte and S. L. Cockroft, *Angew. Chem. Int. Ed.*, 2019,
   58, 12617-12623; b) Q. Y. Wan, J. Yang, W. P. To and C. M. Che, *Proc. Natl. Acad. Sci. USA*, 2021,
   118.
- a) H. Clavier and S. P. Nolan, *Chem. Commun.*, 2010, **46**, 841-861; b) L. Falivene, Z. Cao, A. Petta,
   L. Serra, A. Poater, R. Oliva, V. Scarano and L. Cavallo, *Nat. Chem.*, 2019, **11**, 872-879.
- 19. Reaction of the analogous Hg-bridged diphosphine complex  $[PdCl_2\{Hg(ortho-C_6H_4PPh_2)\}]$  with 0.5 equiv of  $Pd(dba)_2$  was reported to furnish a Pd(0) species  $[Pd\{\eta^2-(ortho-Ph_2PC_6H_4)_2Hg\}\{\eta^1-(ortho-Ph_2PC_6H_4)(ortho-Ph_2P(O)C_6H_4)Hg\}]$  after recrystallization from  $CH_2Cl_2/Et_2O$  without evidence of  $CH_2Cl_2$  activation. See reference 5.
- 20. The coupling constant is consistent with reported values for Pd complexes with different triarylphosphines in a *trans*-geometry. See: P. Cianfriglia, V. Narducci, C. LoSterzo, E. Viola, G. Bocelli and T. A. Kodenkandath, *Organometallics*, 1996, **15**, 5220-5230.
- 21. A. Abo-Amer, M. S. McCready, F. B. Zhang and R. J. Puddephatt, Can. J. Chem., 2012, 90, 46-54.
- 22. P. Leoni, *Organometallics*, 1993, **12**, 2432-2434.
- 23. M. Huser, M. T. Youinou and J. A. Osborn, *Angew. Chem. Int. Ed.*, 1989, **28**, 1386-1388.
- 24. See also: C. A. Ghilardi, S. Midollini, S. Moneti, A. Orlandini and J. A. Ramirez, *J. Chem. Soc., Chem. Commun.*, 1989, 304-306.

- 25. A. Döhring, R. Goddard, G. Hopp, P. W. Jolly, N. Kokel and C. Krüger, *Inorg. Chim. Acta*, 1994, **222**, 179-192.
- 26. K. Mashima, A. Fukumoto, H. Nakano, Y. Kaneda, K. Tani and A. Nakamura, *J. Am. Chem. Soc.*, 1998, **120**, 12151-12152.
- 27. V. A. Zinovyeva, S. Mom, S. Fournier, C. H. Devillers, H. Cattey, H. Doucet, J. C. Hierso and D. Lucas, *Inorg. Chem.*, 2013, **52**, 11923-11933.

# **TOC Entry**



In trigonal LPd $^0$ (dba) complexes with diastereomeric diferrocenylmercury diphosphine ligands the Pd coordination environment and Hg...Pd separation are starkly different. The rate of Pd $^0$  complex formation and their reactivity in the oxidative addition of CH $_2$ Cl $_2$  vary significantly.